Results in Physics 46 (2023) 106264

Contents lists available at ScienceDirect

Results in Physics

journal homepage: www.elsevier.com/locate/rinp

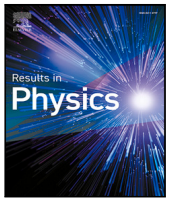

Scheme of non-contact manipulation: Acoustic radiation force on spherical particle in a spherical shell structure

Menyang Gong [a], Xin Xu [a], Yupei Qiao [b], Zhonghan Fei [a], Yuanyuan Li [a], Jiehui Liu [a], Aijun He [c,*], Xiaozhou Liu [a,d,*]

[a] Key Laboratory of Modern Acoustics, Institute of Acoustics and School of Physics, Collaborative Innovation Center of Advanced Microstructures, Nanjing University, Nanjing 210093, China
[b] School of Physics and Electronic Science, Guizhou Normal University, Guiyang 550001, China
[c] School of Electronic Science and Engineering, Nanjing University, Nanjing, 210023, China
[d] State Key Laboratory of Acoustics, Institute of Acoustics, Chinese Academy of Sciences, Beijing 100190, China

ARTICLE INFO

Keywords:
Acoustic tweezers
Acoustic radiation force
Nonlinear acoustics
Non-contact manipulation

ABSTRACT

A theoretical solution of the acoustic radiation force of an arbitrary beam on spherical particles in a spherical shell structure is presented. Taking the bladder and urinary calculus as the background, the finite element simulation of specific parameters was carried out to verify the accuracy and feasibility of the theoretical solution. The variation law of the acoustic radiation force on the particles with the particle radius, incident wave spectrum, viscosity coefficient of the medium inside the spherical shell structure, and distance from the center of the particle to the center of the spherical shell structure is studied. This scheme provides a design idea and theoretical basis for the non-contact manipulation of particles inside the spherical shell structure, and has a wide range of application scenarios in industrial applications and life sciences.

Introduction

In life science and medicine, there is an urgent need for non-invasive and non-contact operation solutions, which can not only reduce the damage to biological tissues, but also greatly reduce the pain of patients. Therefore, acoustic manipulation, as an important way of non-contact manipulation, has recently become the focus of attention. In 1992, Wu et al. proposed the concept of acoustic tweezers [1,2]. The acoustic tweezers based on acoustic radiation force(ARF) have good biological adaptability, and the structural scale manipulated is just between biological macromolecules and biological tissues. Noncontact manipulation of particles and cells with ARF enables a wide array of applications for tissue engineering and biosensing [3]. The calculation of the ARF also revealed a close relationship between the acoustic field and fundamental field properties: gauge momentum and spin angular momentum density [4]. In recent years, the ARF has also been used as a criterion to detect whether the isolated living cells are abnormal [5]. Under free boundary conditions, the ARF of plane wave acting on spherical and cylindrical particles has been calculated [6–10]. The ARF of Gaussian wave and Bessel wave acting on standard particles in ideal fluid has also been studied [11–20]. The calculation method of ARF has been greatly developed in recent years [21–23]. The distribution of the sound field in the structure of the spherical shell is analyzed [24]. In practical biological structures, spherical shell is a common boundary condition, such as bladder. However, the ARF on particles under spherical shell boundary conditions is rarely studied at present. In many practical applications, it is often impossible to place the sound source inside the spherical boundary, and only place the sound source outside the spherical shell structure to emit sound waves, otherwise it violates the principle of non-invasive and non-contact. Therefore, it is of great significance to propose a solution to the ARF exerted by the sound source outside the spherical shell on the particles in the boundary of the spherical shell. There is an urgent need for this law in the life science.

Analysis of sound field and theoretical calculation of acoustics radiation force

Because most application scenarios in spherical shell environment require particles to move along the radius, such as the potential demand to assist in the excretion of urinary stones. Therefore, the model is established as shown in the schematic diagram. The outermost layer is the environmental medium. The spherical shell is a fluid medium, and the incident beam enters from the left side of the picture. The target

* Corresponding authors.
E-mail addresses: haj@nju.edu.cn (A. He), xzliu@nju.edu.cn (X. Liu).

https://doi.org/10.1016/j.rinp.2023.106264
Received 29 November 2022; Received in revised form 31 January 2023; Accepted 3 February 2023
Available online 6 February 2023

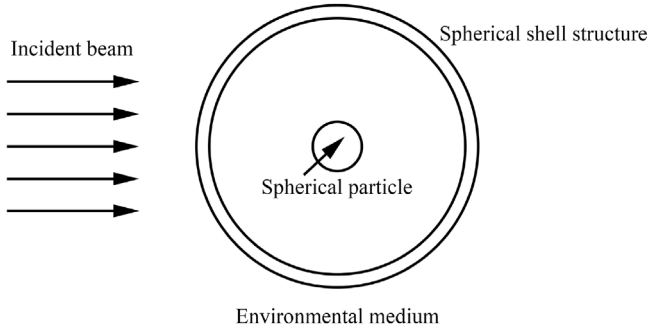

Fig. 1. Sectional view of spherical particle manipulation in a spherical shell based on acoustic radiation force.

spherical particles are placed in the spherical shell medium, and the whole model is rotationally symmetric. Set the outer diameter of the spherical shell structure be R and the inner diameter be R'. The radius of the spherical particle is a (see Fig. 1).

The basic equation of single frequency sound wave is to satisfy the Laplace equation. For that Laplace operator satisfies the superposition principle, it only needs to consider the single frequency beam to cover all cases. When the Gaussian wave and Bessel wave are used as one kind of the incident beams, the spectrum expansion can also be performed during the analysis, and each frequency component can be analyzed independently in the calculation of the acoustic radiation force. Only the plane wave is needed to investigate, so the incident sound pressure is set:

$$\boldsymbol{\Phi}_i = \boldsymbol{\Phi}_0 \sum_{n=0}^{\infty}(2n+1)(i)^n j_n(k_0 r)P_n(cos\theta) \tag{1}$$

here $\boldsymbol{\Phi}_0$ is the incident velocity potential, k_0 is the wavenumber of the sound wave in the external environment medium, j_n is the first kind of spherical Bessel function of order n, P_n is the Legendre function of order n.

Similarly, the scattered wave can also be expanded into a linear combination of spherical waves:

$$\boldsymbol{\Phi}_s = \boldsymbol{\Phi}_0 \sum_{n=0}^{\infty} A_{n,s}(2n+1)(i)^n h_n^{(1)}(k_0 r)P_n(cos\theta) \tag{2}$$

here $A_{n,s}$ is the coefficient of scattered sound wave, h_n is the third kind of spherical Bessel function of order n. For that the sound wave needs to propagate to the interior of the controlled structure, the elastic boundary conditions should be taken between the medium and the structure, and between the middle and layers of the structure. There is mode conversion at the boundary, so the medium particle displacement satisfies the mode conversion equation:

$$\nabla^2 u + \frac{\lambda+\mu}{\mu}\frac{\partial}{\partial t}\nabla(\nabla\cdot u) = \frac{1}{c_s^2}\frac{\partial^2 u}{\partial t^2} \tag{3}$$

here λ and μ are the Lame coefficient, $c_S = \sqrt{\frac{\mu}{\rho_0}}$.

For the spherical shell structure, the velocity potential of longitudinal wave can be expressed as:

$$\begin{aligned}\boldsymbol{\Phi}_1 &= \boldsymbol{\Phi}_c \sum_{n=0}^{\infty}(2n+1)(i)^n[A_{n,1a}j_n(k_{11}r)\\ &\quad + A_{n,1b}h_n^{(1)}(k_{11}r)]P_n(cos\theta)\end{aligned} \tag{4}$$

here $\boldsymbol{\Phi}_c$ is velocity potential constant, n_n is Neumann function, $A_{n,1a}$ and $A_{n,1b}$ are pending parameters, k_{11} is the longitudinal wavenumber in the spherical shell structure.

Transverse wave velocity potential:

$$\begin{aligned}\boldsymbol{\Psi}_1 &= \boldsymbol{\Phi}_c \sum_{n=0}^{\infty}(2n+1)(i)^n[A_{n,1c}j_n(k_{12}r)\\ &\quad + A_{n,1d}h_n^{(1)}(k_{12}r)]\frac{dP_n(cos\theta)}{d\theta}\end{aligned} \tag{5}$$

The interior of the spherical shell is a viscous fluid:

$$\begin{aligned}\boldsymbol{\Phi}_2 &= \boldsymbol{\Phi}_c \sum_{n=0}^{\infty}(2n+1)(i)^n[A_{n,2a}j_n(k_{21}r)\\ &\quad + A_{n,2b}h_n^{(1)}(k_{21}r)]P_n(cos\theta)\\ \boldsymbol{\Psi}_2 &= \boldsymbol{\Phi}_c \sum_{n=0}^{\infty}(2n+1)(i)^n[A_{n,2c}j_n(k_{21}r)\\ &\quad + A_{n,2d}h_n^{(1)}(k_{22}r)]\frac{dP_n(cos\theta)}{d\theta}\end{aligned} \tag{6}$$

Since the shear wave decays rapidly in the fluid, based on numerical calculation, in the general viscosity environment, the mode conversion of the inner boundary of the spherical shell and the mode conversion of the spherical particle surface have little effect on the ARF (the effect on the value is less than 1%), so when calculating the viscosity, it is only necessary to consider the definition formula of the ARF in viscous environments.

In the viscous case the velocity field is not irrotational and should be decomposed into a temperature wavefield, a rotational wavefield, and an acoustic wavefield. Since the main application scenario of the solution is the effect of sound waves on calculus in the bladder, the main environmental medium is urine. Unless special circumstances such as proteinuria occur, the viscosity of the medium is low. The existence of viscosity is the cause of temperature field and rotational wave field. Therefore, the effects of temperature wave field and rotational wave field are ignored here. This approximation should be reasonable, for that the solution obtained based on this theory has little difference with the result obtained by finite element simulation.

The sound field inside the target elastic spherical particle can be expressed as, shear waves should also be taken into account:

$$\begin{aligned}\boldsymbol{\Phi}_3 &= \boldsymbol{\Phi}_c \sum_{n=0}^{\infty}(2n+1)(i)^n[A_{n,3a}j_n(k_{31}r)\\ &+ A_{n,3b}h_n^{(1)}(k_{31}r)]P_n(cos\theta)\\ \boldsymbol{\Psi}_3 &= \boldsymbol{\Phi}_c \sum_{n=0}^{\infty}(2n+1)(i)^n[A_{n,3c}j_n(k_{32}r)\\ &+ A_{n,3d}h_n^{(1)}(k_{32}r)]\frac{dP_n(cos\theta)}{d\theta}\end{aligned} \tag{7}$$

here $A_{n,1a}, A_{n,1c}, A_{n,2a}, A_{n,2c}, A_{n,3a}$ and $A_{n,3c}$ are undetermined scattering parameters, which are uniquely determined by the boundary condition equations. $k_{11}, k_{12}, k_{21}, k_{22}, k_{31}, k_{32}$ are the transverse and longitudinal wave number of each region.

The boundary conditions can be expressed:

$$\begin{aligned}&\upsilon_{0r}|_{r=R} = \upsilon_{1r}|_{r=R}\\ &\upsilon_{0\theta}|_{r=R} = \upsilon_{1\theta}|_{r=R}\\ &\sigma_{0rr}|_{r=R} = \sigma_{1rr}|_{r=R}\\ &\sigma_{0r\theta}|_{r=R} = \sigma_{1r\theta}|_{r=R}\\ &\upsilon_{1r}|_{r=R'} = \upsilon_{2r}|_{r=R'}\\ &\upsilon_{1\theta}|_{r=R'} = \upsilon_{2\theta}|_{r=R'}\\ &\sigma_{1rr}|_{r=R'} = \sigma_{2rr}|_{r=R'}\\ &\sigma_{1r\theta}|_{r=R'} = \sigma_{2r\theta}|_{r=R'}\\ &\upsilon_{2r}|_{r=a} = \upsilon_{3r}|_{r=a}\\ &\upsilon_{2\theta}|_{r=a} = \upsilon_{3\theta}|_{r=a}\\ &\sigma_{2rr}|_{r=a} = \sigma_{3rr}|_{r=a}\\ &\sigma_{2r\theta}|_{r=a} = \sigma_{3r\theta}|_{r=a}\end{aligned} \tag{8}$$

The specific expression of continuity boundary condition is:

$$\upsilon_{0r} = \frac{\partial \boldsymbol{\Phi}_0}{\partial r}$$

$$\upsilon_{0\theta} = \frac{1}{r}\frac{\partial \boldsymbol{\Phi}_0}{\partial \theta}$$

$$\sigma_{0rr} = -\lambda k_L^2 \Phi_0 + 2\mu\{\frac{\partial^2}{\partial r^2}\Phi_0\}$$
$$\sigma_{0r\theta} = \mu\{2\frac{\partial}{\partial r}[\frac{1}{r}\frac{\partial}{\partial \theta}\Phi_0]\}$$
$$v_{1r} = \frac{\partial \Phi_1}{\partial r} + \frac{1}{r\sin\theta}\frac{\Psi_1 \sin\theta}{\partial \theta}$$
$$v_{1\theta} = \frac{1}{r}\frac{\partial \Phi_1}{\partial \theta} - \frac{1}{r}\frac{\partial (r\Psi_1)}{\partial r}$$
$$\sigma_{1rr} = -\lambda k_L^2 \Phi_1 + 2\mu\{\frac{\partial^2}{\partial r^2}[\Phi_1 + \frac{\partial}{\partial r}(r\Psi_1)] + k_t^2(r\Psi_1)\}$$
$$\sigma_{1r\theta} = \mu\{2\frac{\partial}{\partial r}[\frac{1}{r}\frac{\partial}{\partial \theta}[\Phi_1 + \frac{\partial}{\partial r}(r\Psi_1)]] + k_t^2\frac{\partial \Psi_1}{\partial \theta}\}$$
$$v_{2r} = \frac{\partial \Phi_2}{\partial r} + \frac{1}{r\sin\theta}\frac{\Psi_2 \sin\theta}{\partial \theta}$$
$$v_{2\theta} = \frac{1}{r}\frac{\partial \Phi_2}{\partial \theta} - \frac{1}{r}\frac{\partial (r\Psi_2)}{\partial r}$$
$$\sigma_{2rr} = -\lambda k_L^2 \Phi_2 + 2\mu\{\frac{\partial^2}{\partial r^2}[\Phi_2 + \frac{\partial}{\partial r}(r\Psi_2)] + k_t^2(r\Psi_2)\}$$
$$\sigma_{2r\theta} = \mu\{2\frac{\partial}{\partial r}[\frac{1}{r}\frac{\partial}{\partial \theta}[\Phi_2 + \frac{\partial}{\partial r}(r\Psi_2)]] + k_t^2\frac{\partial \Psi_2}{\partial \theta}\}$$
$$v_{3r} = \frac{\partial \Phi_3}{\partial r} + \frac{1}{r\sin\theta}\frac{\Psi_3 \sin\theta}{\partial \theta}$$
$$v_{3\theta} = \frac{1}{r}\frac{\partial \Phi_3}{\partial \theta} - \frac{1}{r}\frac{\partial (r\Psi_3)}{\partial r}$$
$$\sigma_{3rr} = -\lambda k_L^2 \Phi_3 + 2\mu\{\frac{\partial^2}{\partial r^2}[\Phi_3 + \frac{\partial}{\partial r}(r\Psi_3)] + k_t^2(r\Psi_3)\}$$
$$\sigma_{3r\theta} = \mu\{2\frac{\partial}{\partial r}[\frac{1}{r}\frac{\partial}{\partial \theta}[\Phi_3 + \frac{\partial}{\partial r}(r\Psi_3)]] + k_t^2\frac{\partial \Psi_3}{\partial \theta}\} \quad (9)$$

In order to make the expression clearer, here is a review of the process of solving the undetermined coefficients. The method of solving the sound field with undetermined coefficients has been widely used before, which has been proven to be a feasible and effective method [25]. Based on Eq. (8), it can be known that the boundary condition equation could be expressed in terms of v and σ. Based on Eq. (9), it can be known that v and σ could be expressed in terms of Φ and Ψ. Based on Eqs. (4)–(7), it can be known that Φ and Ψ could be expressed by the undetermined coefficients. After this variable substitution, the boundary condition equation represented by the undetermined coefficients could be obtained. The undetermined coefficients are uniquely determined by the boundary condition equations, so that the undetermined coefficients can be solved.

Thus, the velocity potential field information is obtained. By definition, the ARF can be obtained by annular integration of the stress tensor at the surface of a spherical particle:

$$\boldsymbol{F} = \langle \iint_{S_0} \boldsymbol{\sigma} d\boldsymbol{S} \rangle \quad (10)$$

where $\langle\rangle$ is the time average, S_0 is the surface of the spherical particle, and σ is the stress tensor. Here the annular integral refers to the entire surface of the spherical particle. In a viscous fluid, the stress tensor satisfies:

$$\boldsymbol{\sigma} = (-p_1 + \lambda'\nabla \cdot \boldsymbol{v})\boldsymbol{E} + 2\mu'\boldsymbol{e} \quad (11)$$

where $\boldsymbol{E}$ is the unit vector. The deformation rate tensor is:

$$\boldsymbol{e} = \frac{(\nabla \boldsymbol{v}) + (\nabla \boldsymbol{v})^T}{2} \quad (12)$$

where λ' is the expansion viscosity coefficient, and μ' is the dynamic viscosity coefficient. The sound pressure p_1 has an expanded expression:

$$p_1 = \rho_0(\frac{\lambda' + 2\mu'}{\rho_0}\Delta - \frac{\partial}{\partial t})\Phi_2 + \frac{\rho_0}{2c_0}(\frac{\partial \Phi_2}{\partial t}) - \frac{1}{2}\rho_0(\nabla\Phi_2)^2 - \frac{\lambda' + 2\mu'}{c_0^2}\frac{\partial \Phi_2}{\partial t}\Delta\Phi_2 \quad (13)$$

Thereby, the ARF on spherical particles in the viscous medium in the spherical shell structure is obtained. Based on the superposition principle, the ARF of complex incident waves can be obtained by linear superposition of the ARF generated by single frequency waves obtained from spectral analysis.

Since spherical particles are located in the center of the spherical shell structure only in some cases, and spherical particles at the center of the sphere also move when subjected to the ARF, the migration is also included in the discussion in the subsequent discussion. When the spherical particles are offset from the center of the spherical shell structure, since the topological structure of the nesting does not change, it can be processed in the same way by means of coordinate transfer [21–23].

Table 1
Parameters selection of medium.

Parameter	Symbols	Numerical value
The inner radius of the spherical shell	R'	2.75 mm
The outer radius of the spherical shell	R	3 mm
Sound speed of external fluid	c_{IF}	1580 m/s
Density of external fluid	ρ_{IF}	$1.054 * 10^3$ kg/m^3
Sound speed of fluid inside the spherical shell	c_0	1480 m/s
Density of fluid inside the spherical shell	ρ_0	$1.010 * 10^3$ kg/m^3
Dynamic viscosity coefficient of fluid inside the spherical shell	μ'	$2.98 * 10^{-3}$ Pa s
Expansion viscosity coefficient of fluid inside the spherical shell	λ'	$2.4 * 10^{-3}$ Pa s
Density of spherical shell	ρ_u	$1.1 * 10^3$ kg/m^3
Young's modulus of spherical shell	E_{ru}	0.3 MPa
Poisson ratio of spherical shell	ν_u	0.49
Density of spherical particle	ρ_{MO}	$2.2 * 10^3$ kg/m^3
Young's modulus of spherical particle	E_{rMO}	2.65 GPa
Poisson ratio of spherical particle	ν_{MO}	0.41

Verification, analysis and interpretation based on theoretical calculation and finite element simulation

In order to verify the correctness of the algorithm and the feasibility of this approach, theoretical calculations based on the algorithm proposed in the previous section and finite element simulations based on COMSOL are carried out. Incident sound waves enter from above. The structure shown as a cylinder is the external medium, and the boundaries are set as all perfectly matched layers. Theoretical calculations and finite element simulations are performed in the context of pushing the movement of urinary calculus in the bladder, so the parameters are selected as shown in Table 1. Unless otherwise specified, the theoretical solutions and finite element simulations calculated in this section are based on Table 1.

Variation of the acoustic radiation force with the radius of spherical particles

Due to the differences in the size of the manipulated particles, to verify that the proposed algorithm has good prediction results for particles of various radii, theoretical calculations and finite element simulations are carried out. As shown in Fig. 2, the trend of the ARF with the particle radius is more accurately estimated. The absolute amplitude of the incident wave is 1 Pa. The frequency of the incident wave is 1 MHz. The spherical particles have a radius of 0.8 mm to 1.2 mm. The solid black line in the figure is the theoretical solution, and the blue diamond points are the results of the finite element simulation. Fig. 3 shows the sound field distribution when spherical particles with radii of 0.8 mm, 0.9 mm, 1.0 mm, 1.1 mm and 1.2 mm are subjected to the ARF. The absolute amplitude of the incident wave is 1 Pa. The frequency of the incident wave is 1 MHz.

Variation of the acoustic radiation force with incident beam spectrum

Since most sound beams are not single-frequency waves, in actual operation, the incident ARF frequency corresponding to the maximum ARF is expected to be obtained. Therefore, it is necessary to investigate

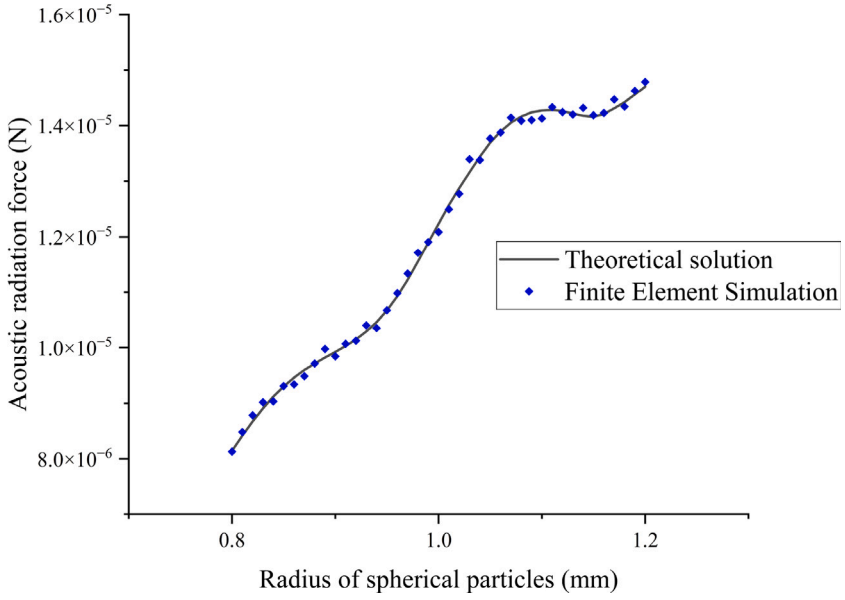

Fig. 2. The acoustic radiation force changing with the radius of spherical particles.

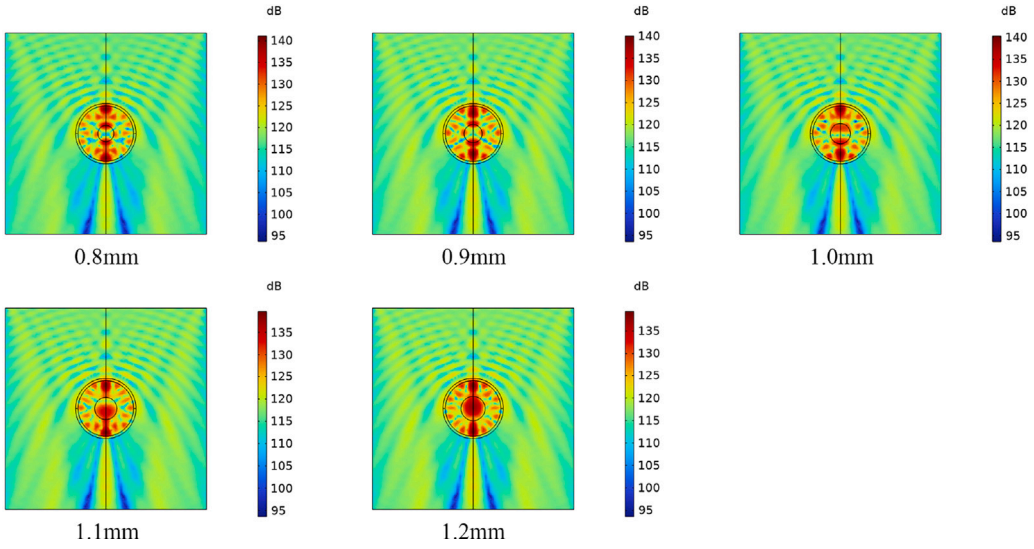

Fig. 3. The sound field distribution when the particle with a radius of 0.8 mm, 0.9 mm, 1.0 mm, 1.1 mm and 1.2 mm, respectively is subjected to the acoustic radiation force.

the ARF on spherical particles under the incident sound beam of different frequencies. As shown in Fig. 4, the trend of the ARF changing with the frequency spectrum of the incident acoustic wave is more accurately estimated. The incident wave has a spectral range of 0.8 MHz to 1.2 MHz. The solid black line in the figure is the theoretical solution, and the blue diamond point is the result of the finite element simulation. Fig. 5 shows the sound field distribution of spherical particles when the incident wave spectrum is 0.8 MHz, 0.9 MHz, 1.0 MHz, 1.1 MHz, and 1.2 MHz when the ARF is applied. The absolute amplitude of the incident wave is 1 Pa. By analyzing the frequency spectrum, suitable frequency bands could be selected so that the particles are subjected to the maximum ARF, thereby improving the efficiency of particle manipulation.

Variation of the acoustic radiation force with fluid viscosity in spherical shell

Since the medium in the spherical shell is changeable, especially in life sciences, the parameters of body fluids are usually not fixed, but are in an adjustable range. Therefore, the ARFs on spherical particles with different viscosity coefficients are studied. As shown in Fig. 6, the ARF is plotted as a function of the viscosity coefficient. The absolute amplitude of the incident wave is 1 Pa. The frequency of the incident wave is 1 MHz. The dynamic viscosity coefficient and the expansion viscosity coefficient of fluid vary from $2.0 * 10^{-3}$ Pa s to $3.0 * 10^{-3}$ Pa s.

Variation of the acoustic radiation force with the distance of spherical particles away from the center of spherical shell structure

For that in some cases, spherical particles are not in the center of the spherical shell structure. During the manipulation of spherical particles, the spherical particles are also offset from the center of the spherical shell structure. At the same time, in order to explore the variation of the ARF on the spherical particles during the operation process, the variation law of the ARF on the particles with the offset distance between the particle and the center of the spherical shell structure is plotted in Fig. 7. The absolute amplitude of the incident wave is 1 Pa. The frequency of the incident wave is 1 MHz. It can be clearly seen that

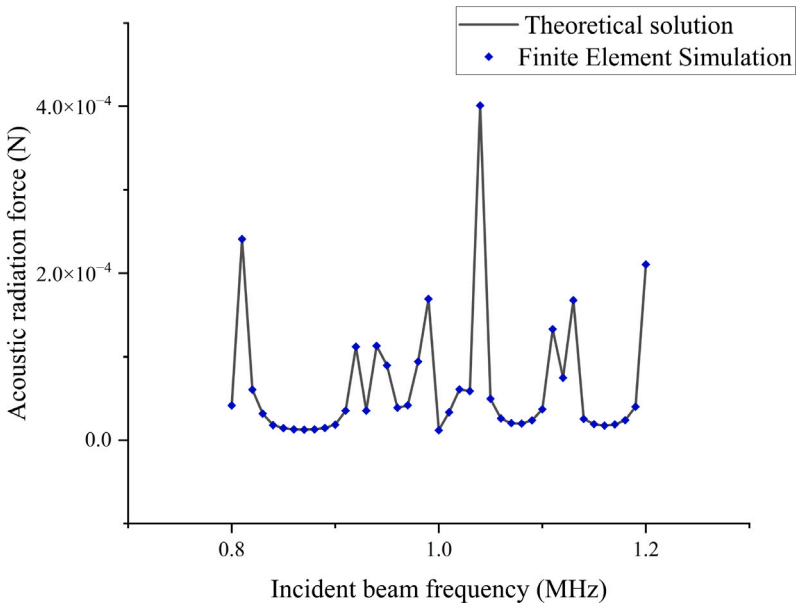

Fig. 4. The acoustic radiation force changing with the incident beam frequency.

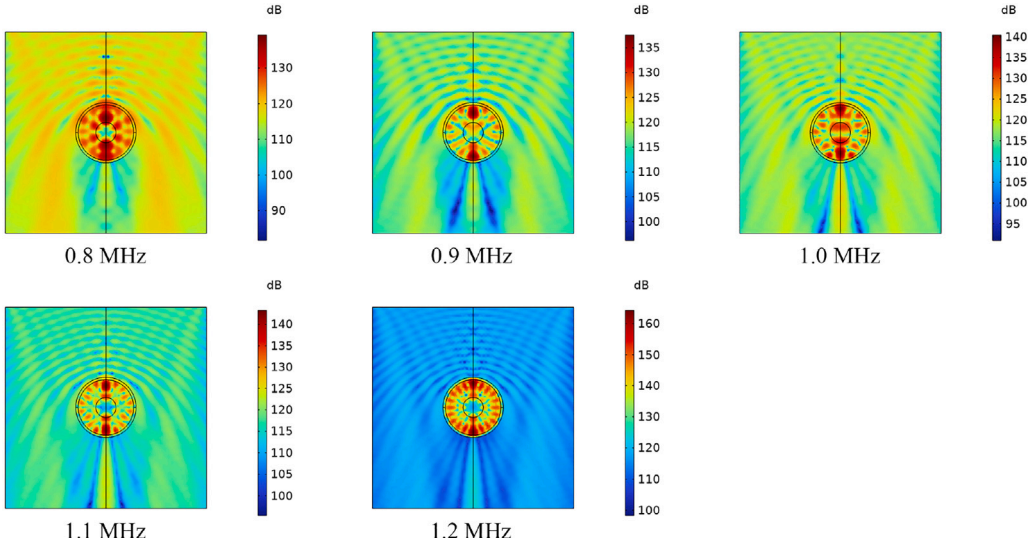

Fig. 5. The sound field distribution when the particle is subjected to the acoustic radiation force of the incident sound wave with a frequency of 0.8 MHz, 0.9 MHz, 1.0 MHz, 1.1 MHz, and 1.2 MHz, respectively.

there are two distinct peaks when the spherical particles move forward and backward to the spherical shell, which we think is caused by the resonance structure formed by the spherical particles and the spherical shell structure. The distance has a spectral range of −1.5 mm to 1.5 mm. Fig. 8 shows the sound field distribution of spherical particles when the distance of spherical particles away from the center of spherical shell structure is −1.5 mm, −1.0 mm, −0.5 mm, 0 mm, 0.5 mm, 1.0 mm and 1.5 mm when the ARF is applied. The absolute amplitude of the incident wave is 1 Pa. The frequency of the incident wave is 1 MHz. In more detail, the transformation of the sound field distribution during the axial movement of the spherical particles by the ARF can be seen in the animation S1 of the supplementary material. The four formants of Fig. 8 can be seen intuitively and clearly in the animation S1.

Generally speaking, the direction of the incident beam can be adjusted. Based on the symmetry of the model, the incident direction of the incident beam only needs to be selected parallel to the line connecting the center of the spherical particle and the center of the outer spherical shell, and the model can be transformed into the situation outlined in the animation S1.

In the case of non-standard spherical particles, due to the reduced symmetry and the need to consider factors such as particle rotation, it is relatively difficult to directly calculate the ARF analytically. This is also the computational research work which need to be carried out next. However, the results of the spherical particles obtained in the manuscript still have reference significance for the force on the quasi-spherical particles, and the quasi-spherical particles will also be subjected to acoustic radiation force similar to that of the standard spherical particles. Within the allowable range of error, we can treat the quasi-spherical particles as spherical particles. The particles will also be pushed by the acoustic radiation force, but the results will have some errors.

By adjusting the intensity, incident direction and frequency of the incident sound beam, the spherical particles in the spherical shell structure can be moved at a specified acceleration and reached to any specified position in the spherical shell.

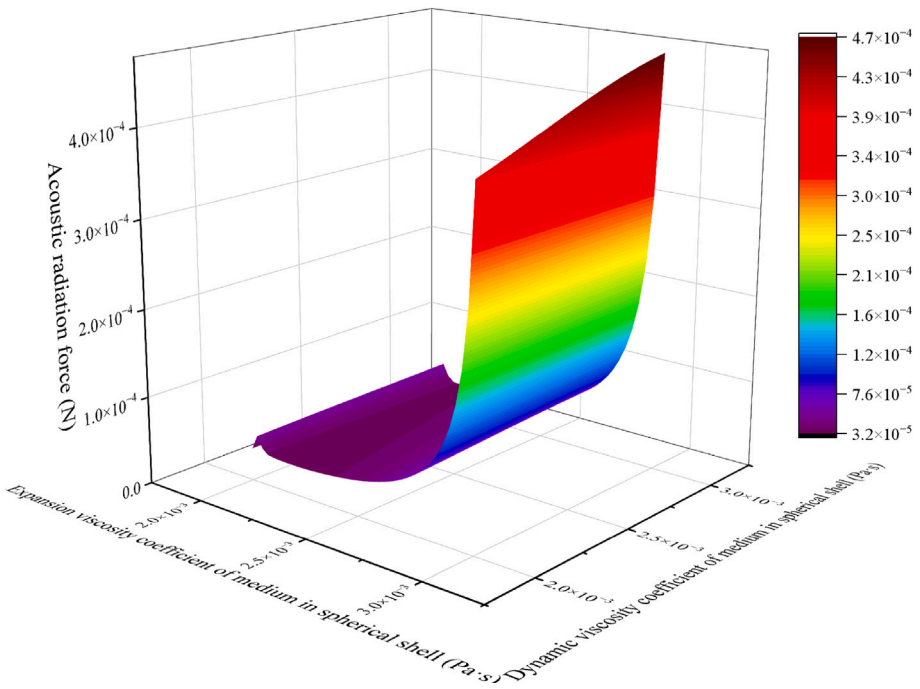

Fig. 6. The acoustic radiation force changing with fluid viscosity in spherical shell.

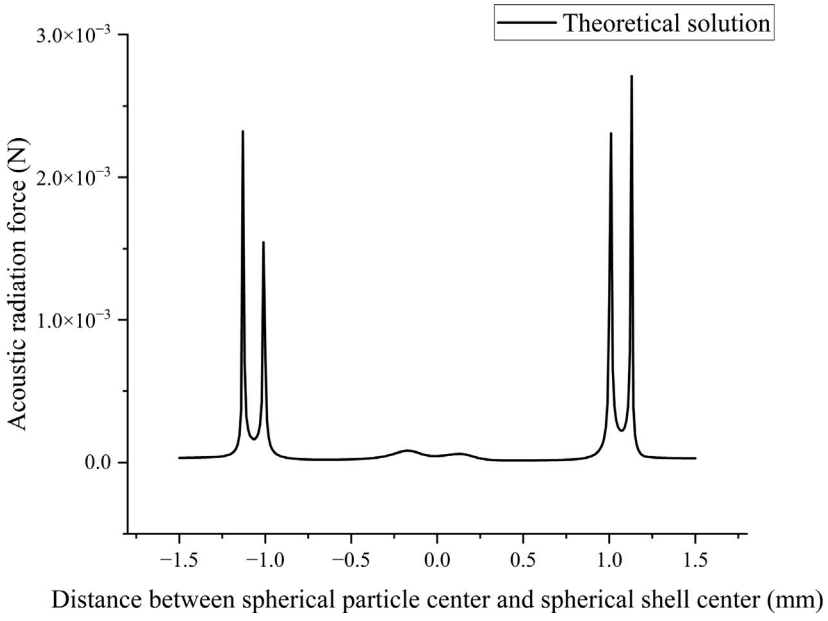

Fig. 7. The acoustic radiation force changing with the distance of spherical particles away from the center of spherical shell structure.

Conclusion

In this paper, an acoustic radiation force scheme for non-contact manipulation of particles inside a spherical shell structure is proposed. The accuracy and feasibility of the solution are verified by the finite element method. The influences of parameters such as the radius of spherical particles, the frequency spectrum of incident acoustic waves, the viscosity of the medium inside the spherical shell, and the offset distance between the spherical particles and the spherical center of the spherical shell structure on the acoustic radiation force are analyzed. The spherical shell structure is a common structure in the biological world and industrial production, so it has important application prospects in the fields of life science and industry.

Declaration of competing interest

The authors declare that they have no known competing financial interests or personal relationships that could have appeared to influence the work reported in this paper.

Data availability

Data will be made available on request.

Acknowledgments

Project supported by National Key R&D Program of China (No. 2020YFA0211400), State Key Program of National Natural Science of

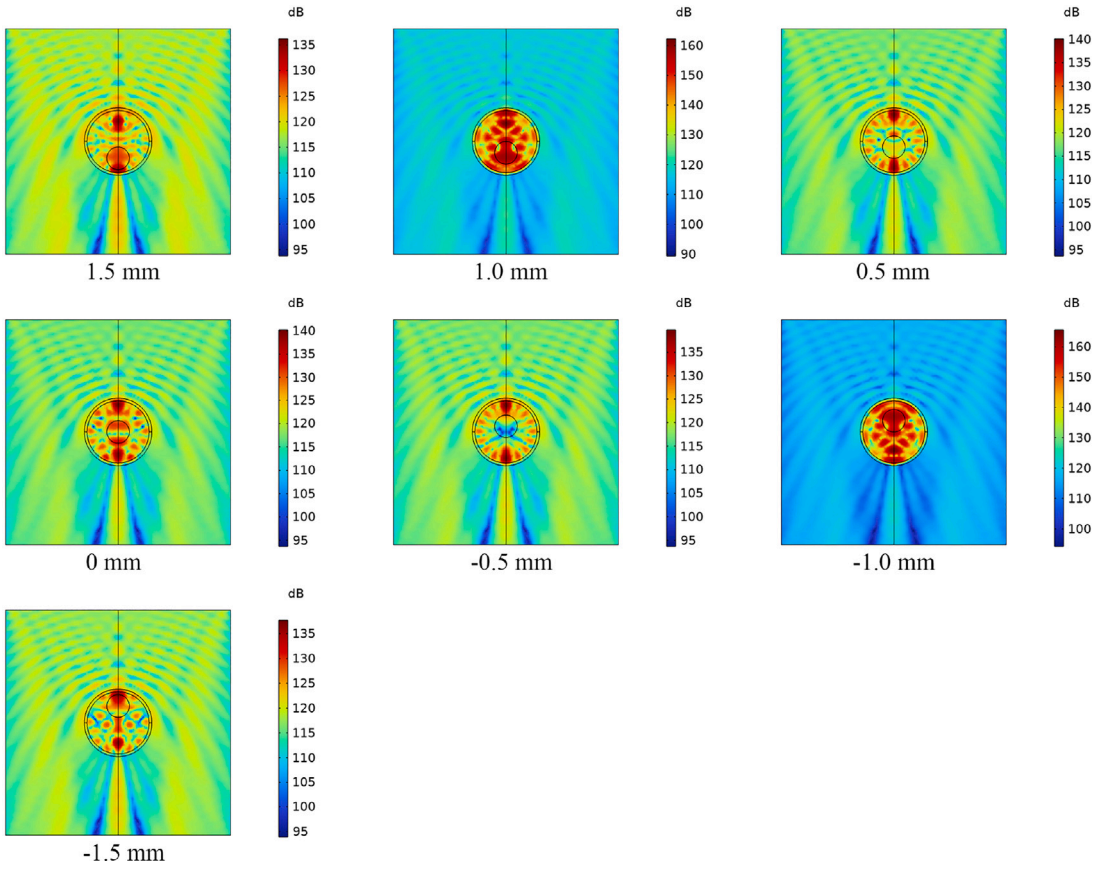

Fig. 8. The sound field distribution when the distance of spherical particles away from the center of spherical shell structure is −1.5 mm, −1.0 mm, −0.5 mm, 0 mm, 0.5 mm, 1.0 mm and 1.5 mm, respectively.

China (No. 11834008), the National Natural Science Foundation of China (No. 12174192), State Key Laboratory of Acoustics, Chinese Academy of Sciences (No. SKLA202210) and Key Laboratory of Underwater Acoustic Environment, Chinese Academy of Sciences (No. SSHJ-KFKT-1701).

Data availability statement

The data that support the findings of this study are available from the corresponding author upon reasonable request.

Supplementary data

Supplementary material related to this article can be found online at https://doi.org/10.1016/j.rinp.2023.106264.

References

[1] Wu JR. Acoustical tweezers. J Acoust Soc Am 1991;89(5):2140–3.
[2] Wu JR, Du GH. Acoustic radiation force on a small compressible sphere in a focused beam. J Acoust Soc Am 1990;87(3):997–1003.
[3] Urban MW. Production of acoustic radiation force using ultrasound: methods and applications. Expert Rev Med Dev 2018;15(11):819–34.
[4] Toftul ID, Bliokh KY, Petrov MI, Nori F. Acoustic radiation force and torque on small particles as measures of the canonical momentum and spin densities. Phys Rev Lett 2019;123(18):183901.
[5] Wang HB, Qiao YP, Liu JH, Jiang B, Zhang GT, Zhang CW, Liu XH. Experimental study of the difference in deformation between normal and pathological, renal and bladder, cells induced by acoustic radiation force. Eur Biophys J Biophys Lett 2020;49(2):155–61.
[6] Marston PL. Comment on "radiation forces and torque on a rigid elliptical cylinder in acoustical plane progressive and (quasi) standing waves with arbitrary incidence" [Phys. Fluids 28, 077104 (2016)]. Phys Fluids 2017;29(2):029101.
[7] Mitri FG. Radiation forces and torque on a rigid elliptical cylinder in acoustical plane progressive and (quasi) standing waves with arbitrary incidence. Phys Fluids 2016;28(7):077104.
[8] Qiao YP, Gong MY, Wang HB, Lan J, Liu T, Liu JH, Mao YW, He AJ, Liu XZ. Acoustic radiation force on a free elastic sphere in a viscous fluid: Theory and experiments. Phys Fluids 2021;33(4):047107.
[9] Qiao YP, Zhang XW, Gong MY, Wang HB, Liu XZ. Acoustic radiation force and motion of a free cylinder in a viscous fluid with a boundary defined by a plane wave incident at an arbitrary angle. J Appl Phys 2020;128(4):044902.
[10] Sapozhnikov OA, Bailey MR. Radiation force of an arbitrary acoustic beam on an elastic sphere in a fluid. J Acoust Soc Am 2013;133(2):661–76.
[11] Gong MY, Qiao YP, Fei ZH, Li YY, Liu JH, Mao YW, He AJ, Liu XZ. Non-diffractive acoustic beams produce negative radiation force in certain regions. AIP Adv 2021;11(6):065029.
[12] Gong MY, Qiao YP, Lan J, Liu XZ. Far-field particle manipulation scheme based on X wave. Phys Fluids 2020;32(11):117104.
[13] Gong ZX, Marston PL, Li W, Chai YB. Multipole expansion of acoustical Bessel beams with arbitrary order and location. J Acoust Soc Am 2017;141(6):El574–8.
[14] Marston PL. Axial radiation force of a Bessel beam on a sphere and direction reversal of the force. J Acoust Soc Am 2006;120(6):3518–24.
[15] Marston PL. Radiation force of a helicoidal Bessel beam on a sphere. J Acoust Soc Am 2009;125(6):3539–47.
[16] Wang HB, Gao S, Qiao YP, Liu JH, Liu XZ. Theoretical study of acoustic radiation force and torque on a pair of polymer cylindrical particles in two Airy beams fields. Phys Fluids 2019;31(4):047103.
[17] Wu RR, Cheng KX, Liu XZ, Liu JH, Gong XF, Li YF. Study of axial acoustic radiation force on a sphere in a Gaussian quasi-standing field. Wave Motion 2016;62:63–74.
[18] Wu RR, Cheng KX, Liu XZ, Liu JH, Gong XF, Li YF. Study of axial acoustic radiation force on a sphere in a Gaussian quasi-standing field. Wave Motion 2016;62:63–74.
[19] Wu RR, Cheng KX, Liu XZ, Liu JH, Mao YW, Gong XF. Acoustic radiation force on a double-layer microsphere by a Gaussian focused beam. J Appl Phys 2014;116(14):144903.
[20] Zhang LK, Marston PL. Axial radiation force exerted by general non-diffracting beams. J Acoust Soc Am 2012;131(4):El329–35.

[21] Gong ZX, Marston PL, Li W. T-matrix evaluation of three-dimensional acoustic radiation forces on nonspherical objects in Bessel beams with arbitrary order and location. Phys Rev E 2019;99(6):063004.
[22] Rong B, Lu K, Rui XT, Ni XJ, Tao L, Wang GP. Nonlinear dynamics analysis of pipe conveying fluid by riccati absolute nodal coordinate transfer matrix method. Nonlinear Dynam 2018;92(2):699–708.
[23] Gong ZX, Marston PL, Li W. T-matrix evaluation of three-dimensional acoustic radiation forces on nonspherical objects in Bessel beams with arbitrary order and location. Phys Rev E 2019;99(6):063004.
[24] Gaunaurd GC, Werby MF. Sound scattering by resonantly excited, fluid-loaded, elastic spherical-shells. J Acoust Soc Am 1991;90(5):2536–50.
[25] Wang YY, Yao J, Wu XW, Wu DJ, Liu XJ. Influences of the geometry and acoustic parameter on acoustic radiation forces on three-layered nucleate cells. J Appl Phys 2017;122(9):094902.